Gas-Phase Protonation Thermochemistry of Adenosine

ARTICLE *in* THE JOURNAL OF PHYSICAL CHEMISTRY B · SEPTEMBER 2008

Impact Factor: 3.3 · DOI: 10.1021/jp804786e · Source: PubMed

3 AUTHORS:

David Touboul
Natural Product Chemistry Institute
118 PUBLICATIONS **1,991** CITATIONS
SEE PROFILE

Guy Bouchoux
Université Paris-Sud 11
231 PUBLICATIONS **2,804** CITATIONS
SEE PROFILE

Renato Zenobi
ETH Zurich
456 PUBLICATIONS **13,073** CITATIONS
SEE PROFILE

Gas-Phase Protonation Thermochemistry of Adenosine

David Touboul,[†] Guy Bouchoux,*[,‡] and Renato Zenobi[†]

Department of Chemistry and Applied Biosciences, ETH Zürich, CH-8093 Zürich, Switzerland, and Laboratoire des Mécanismes Réactionnels, Ecole Polytechnique, 91128 Palaiseau, France

Received: May 30, 2008; Revised Manuscript Received: July 10, 2008

The goal of this work was to obtain a detailed insight on the gas-phase protonation energetic of adenosine using both mass spectrometric experiments and quantum chemical calculations. The experimental approach used the extended kinetic method with nanoelectrospray ionization and collision-induced dissociation tandem mass spectrometry. This method provides experimental values for proton affinity, PA(adenosine) = 979 ± 1 kJ·mol^{-1}, and for the "protonation entropy", $\Delta_p S°$(adenosine) = $S°$(adenosineH$^+$) − $S°$(adenosine) = −5 ± 5 J·mol^{-1}·K^{-1}. The corresponding gas-phase basicity is consequently equal to: GB(adenosine) = 945 ± 2 kJ·mol^{-1} at 298K. Theoretical calculations conducted at the B3LYP/6-311+G(3df,2p)//B3LYP/6-31+G(d,p) level, including 298 K enthalpy correction, predict a proton affinity value of 974 kJ·mol^{-1} after consideration of isodesmic proton transfer reactions with pyridine as the reference base. Moreover, computations clearly showed that N3 is the most favorable protonation site for adenosine, due to a strong internal hydrogen bond involving the hydroxyl group at the 2′ position of the ribose sugar moiety, unlike observations for adenine and 2′-deoxyadenosine, where protonation occurs on N1. The existence of negligible protonation entropy is confirmed by calculations (theoretical $\Delta_p S°$(adenosine) ∼ −2/−3 J·mol^{-1}·K^{-1}) including conformational analysis and entropy of hindered rotations. Thus, the calculated protonation thermochemical properties are in good agreement with our experimental measurements. It may be noted that the new PA value is ∼10 kJ·mol^{-1} lower than the one reported in the National Institute of Standards and Technology (NIST) database, thus pointing to a correction of the tabulated protonation thermochemistry of adenosine.

I. Introduction

Nucleotides are the structural units of ribonucleic acid (RNA) and deoxyribonucleic acid (DNA), containing the genetic code of each organism. Nucleotides are composed of two different parts: a nucleoside and one (or more) phosphate group(s). Nucleosides (adenosine, guanosine, thymidine, cytidine and uridine) are composed of a nucleobase (adenine (Scheme 1A), guanine, thymine, cytosine and uracil, respectively) attached to a ribose or a deoxyribose. Nucleobase moieties of DNA and RNA are directly involved in the formation and the stability of the well-known double helix structure, due to strong hydrogen bounds.[1] Nucleosides can also play roles in different biochemical processes. In this regards, one of the most important nucleoside is certainly adenosine (Scheme 1B) which is directly implied in the energy transfer, as adenosine monophosphate (AMP), diphosphate (ADP) and triphosphate (ATP);[2] in signal transduction,as cyclicAMP;[3] and in redox reactions, with nicotinamide adenine dinucleotide (NAD)[4] or flavin adenine dinucleotide (FAD).[5] All these reactions involve proton or cation transfers, the understanding of which, at the molecular level, passes through the knowledge of the precise site of protonation, changes of conformation upon protonation, and protonation thermochemistry. In solution, experimental ionization constants, *i.e.*, pK_a determination, are easily measured by pH titration and are thus well documented.[6] In contrast, intrinsic structural and thermochemical information, *i.e.*, without solvent, on protonated nucleosides are scarce.

SCHEME 1: Chemical Structures of Adenine (A) and Adenosine (B)

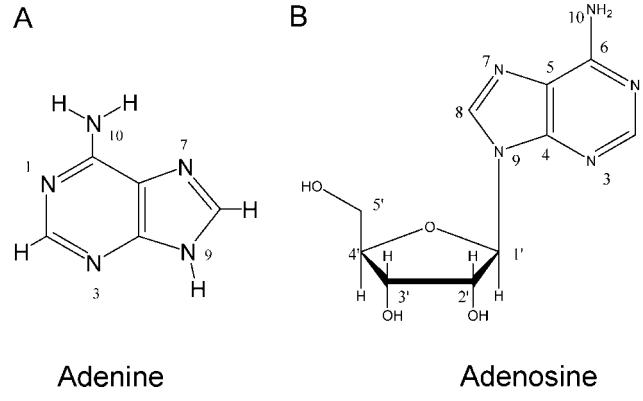

Only very limited experimental data on the protonation thermochemistry of adenosine and its derivates is available in the literature. In 1975, Wilson and McCloskey examined adenosine using chemical ionization with a variety of reactants (methane, isobutane, ammonia, methylamine, dimethylamine and trimethylamine).[7] Using the bracketing method, they estimated that the gas-phase basicity, GB, of adenosine is larger than that of trimethylamine, *i.e.*, 918.1 kJ/mol using the Hunter and Lias[8] recommended GB values. More recently, measurements on adenosine were described by the group of Sindona,[9,10] using the so-called "simple kinetic method".[11] The protonated adducts MHB$^+$ (M = adenosine, *B* = pyrrolidine and piperidine) were produced in a fast atom bombardment (FAB) ion source and the metastable ion dissociations were examined by mass-analyzed ion kinetic energy (MIKE) experiments. After cor-

* Corresponding author. E-mail: bouchoux@dcmr.polytechnique.fr. Telephone: 33 1 69 33 48 42. Fax: 33 1 69 33 48 03.
[†] Department of Chemistry and Applied Biosciences, ETH Zürich.
[‡] Laboratoire des Mécanismes Réactionnels, Ecole Polytechnique.

10.1021/jp804786e CCC: $40.75
Published on Web 08/23/2008

rection to the presently accepted proton affinity scale, the proton affinity values proposed by the authors for adenosine was 989.3 kJ/mol.[10] It has been demonstrated latter[10] that the simple kinetic method used by Greco et al.[9] only leads to the measurement of an apparent proton affinity PA_{app} rather than the true proton affinity at 298 K (PA_{298}). For example, a difference of ca. 10 kJ/mol is observed between two experimental proton affinity values determined by Mautner,[12] using the equilibrium method, and Greco et al.[9] using the simple kinetic method, for adenine, the base involved in adenosine. These two determinations may be reconciled after re-examination of the Greco's data, particularly by considering the difference between PA_{app} and PA_{298} (see Supporting Information S1). It is evident that a similar shift may also occur between the apparent proton affinity of adenosine[10a] (989.3 kJ/mol) recalled above and the true value. To clarify this point, experiments using another method of determination of the protonation thermochemistry of adenosine are consequently needed.

Over the last 15 years, several studies have reported proton affinity calculations of nucleobases using density functional theory (DFT) or Møller−Plesset perturbation theory (MP2).[13] In the case of adenine, preferential protonation on N1 is generally assumed in solution and in the gas phase even though the calculated proton affinity values of N1 and N3 are very close.[14] Very recently, the first calculation of the proton affinity of deoxynucleosides was reported using a geometry optimization at the B3LYP/6-31G* level and a single point calculation with a larger 6-311+G** basis set.[15] To the best of our knowledge, no theoretical investigation on the protonation of adenosine at a comparable level of theory has been undertaken.

We decided to fill this lack of definitive experimental and theoretical data for the proton thermochemistry of adenosine. First, most of the drawbacks of the simple kinetic method may be removed by using its "extended" version.[11] Moreover, the extended kinetic method not only provide the 298K proton affinity but also a "protonation entropy", as defined by the difference $\Delta_p S°_{298} = S°_{298}(MH^+) - S°_{298}(M)$, this later being presently lacking. We thus experimentally re-examined the gas-phase proton thermochemistry of adenosine, using the "extended kinetic method". Second, calculations of the protonation thermochemistry of adenosine, *i.e* PA_{298} and $\Delta_p S°_{298}$, were conducted using the DFT approach at the B3LYP/6-311+G(3df,2p)//B3LYP/6-31+G(d,p) level corrected to a temperature of 298 K and isodesmic proton-transfer reactions referenced to pyridine.

II. Experimental and Computational Methods

Adenosine, the reference bases B_i (dinpropylamine, diisopropylamine, triethylamine, and tripropylamine), and methanol were all purchased from Sigma (Sigma-Aldrich Chemie GmbH, Buchs, Switzerland). Adenosine was dissolved in a water/methanol/acetic acid mixture (50/50/0.1, V/V/V) at a final concentration of 100 μM. Then, 1 μL of the base was added to a 100 μL adenosine stock solution.

ESI-MS spectra were acquired on a hybrid quadrupole time-of-flight mass spectrometer (Q-ToF Ultima, Waters, Manchester, U.K.) equipped with an automated chip-based nanoESI system (Nanomate 100, Advion Biosciences, Ithaca, NY). The mass spectrometer was tuned with gentle desolvation parameters to keep the proton-bond dimers intact during their transfer from solution to the gas phase. The settings used were 45 V for the cone voltage, 50 V for RF1 and −3 V for the ion guide. The source temperature was set to 50 °C. Collision induced dissociation (CID) spectra were obtained using argon as collision gas at a fixed pressure estimated to $\sim 10^{-3}$ mbar and for different values of the collision energy in the laboratory frame, $E_{laboratory}$. It was assumed that $E_{laboratory}$ is directly related to the voltage difference between the ion guide and the gas cell, which is defined as the sum of the static offset value (so-called "collision energy" parameter) and the ion guide value. Thus, the range of $E_{laboratory}$ that was explored was between 5 and 25 eV. The center of mass collision energy, E_{cm}, was deduced using the usual conversion expression: $E_{cm} = E_{laboratory} \times m_{target}/(m_{target} + m_{ion})$. Acquisition times were optimized to obtain sufficient signal intensity (approximately 30 s). The CID mass spectra, obtained for each $[adenosine + H + B_i]^+$ proton bound dimer at various E_{cm}, were examined using the so-called "extended kinetic method" (see below for a complete description of this method). The $[MH]^+$ and $[B_iH]^+$ intensities were evaluated by summing the fragment ion abundances of each protonated species. This procedure should be valid when no further excitation energy is given to the produced fragment ions in the collision cell. Finally, the data were treated using the ODRPACK program for weighted orthogonal distance regression.[11h,16]

Molecular orbital calculations were performed with density functional theory using the GAUSSIAN03 suite of programs.[17] Geometries were optimized using the B3LYP hybrid functional and the 6-31G(d,p) and 6-31+G(d,p) basis sets. Local minima were characterized by harmonic frequencies calculations at these levels (all real frequencies). The unscaled B3LYP/6-31+G(d) frequencies and moments of inertia were used to calculate thermal correction to enthalpy at 298 K. Improved energies were obtained by single point calculations at the B3LYP/6-311+G(3df,2p)//B3LYP/6-31+G(d,p) and B3LYP/6-311++G(3df,2p)//B3LYP/6-31+G(d,p) levels. An isodesmic procedure was finally used to correct for the remaining deficiencies of the DFT formalism in predicting proton affinities.[18]

III. Results and Discussion

Computational Strategy and Adenine As Starting Material. Since our goal was to examine a glycosylated derivative of adenine, *i.e*, adenosine, we have to choose a computational approach that is applicable to large molecules and yields accurate proton affinities without a prohibitive time cost. The computational strategy adopted in the present work relies on a density functional DFT approach.[19] Geometries were first optimized at the B3LYP/6-31G(d,p) level in order to explore a large part of the conformational space of the various neutral and protonated systems. The most important structures were then explored more deeply with the 6-31+G(d,p) and 6-311++G(3df,2p) basis sets (B3LYP/6-31+G(d,p)//B3LYP/6-31+G(d,p) harmonic frequencies and B3LYP/6-311++G(3df,2p)//B3LYP/6-31+G(d,p) energies).

For an accurate calculation of proton affinities the role of diffuse functions on the heavy atoms is essential. This point has been underlined recently by Yao et al.[20] and may be emphasized here for three simple molecules, namely pyridine, pyrimidine and 2-aminopyridine. Their protonation thermochemistry may serve as a model for adenine and adenosine, since protonation occurs on the same types of nitrogen atoms in these molecules. The proton affinities calculated for these molecules at the B3LYP/6-31G(d,p)//B3LYP/6-31G(d,p), B3LYP/6-31+G(d,p)//B3LYP/6-31+G(d,p), and B3LYP/6-311++G(3df,2p)//B3LYP/6-31+G(d,p) levels are summarized in Table 1. The difference between the results obtained with the 6-31G(d,p) and the 6-31+G(d,p) basis sets is quite surprising. Our results thus confirm the findings of Yao et al.[20] that the calculated proton affinity appears to be overestimated (here by 18−25 kJ/mol) when the used basis set does not include diffuse functions.

TABLE 1: Calculated 298 K Proton Affinities of Reference Compounds and Adenine (in kJ/mol)

	pyridine	pyrimidine	2-aminopyridine	adenine (N_1)
B3LYP/6-31G(d,p)[a]	954.4	908.9	979.1	971.1
B3LYP/6-31+G(d,p)[a]	936.0	890.6	955.4	944.5
B3LYP/6-311++G (3df,2p)[b]	936.7	893.5	957.5	949.0
experiment[c]	928.8	885.8	947.2	939.1
iso6-31G(d,p)[d]	928.8	883.3	953.4	945.5
iso6-31+G(d,p)[d]	928.8	883.4	948.2	937.3
iso6-311++G(3df,2p)[d]	928.8	885.6	949.6	941.1

[a] Geometry optimized and vibrational contribution calculated at this level. [b] On B3LYP/6-31G(d,p) optimized geometries. [c] See text for the relevant literature and comments. [d] Isodesmic proton affinities calculated with reference to PA(pyridine) = 928.8 kJ/mol.

Second, no significant change is observed if a larger basis set is employed. The proton affinities calculated at the B3LYP/6-311++G(3df,2p)//B3LYP/6-31+G(d,p) level are not significantly different from those obtained at the B3LYP/6-31+G(d,p)//B3LYP/6-31+G(d,p) level. Finally, if a comparison is made with the currently available experimental proton affinities, it appears that all B3LYP computations lead to an overestimate of the proton affinities of ca. 8 kJ/mol for the set of simple molecules studied here.

Two possibilities exist to remove this systematic deviation. The first one is to use higher level computations such as for example the composite procedures G3,[21] G3B3,[22] or CBS-QB3,[23] which include various post Hartree−Fock calculations in the form of additive corrections. Unfortunately, the cost of such expensive procedures is prohibitive for systems as large as adenosine. The second possibility is to consider an isodesmic reaction[18] of the type: $MH^+ + B \rightarrow M + BH^+$. Accordingly, it is expected that if the same numbers of bonds of the same type are present on both sides of the reaction, systematic deviations cancel. A corrected, "isodesmic", proton affinity for the molecule of interest M may be thus deduced by anchoring the computed enthalpy of the reaction above to the experimental proton affinity of a reference: $PA_{isodesmic}(M) = PA_{exp}(reference) + \Delta_1 H°_{298\ theoretical}$. This procedure was applied to pyrimidine, 2-aminopyridine and adenine, using pyridine as reference in Table 1. We use pyridine since its protonation thermochemistry has already been well described.[7] In particular, Mautner and Sieck obtained an accurate value for the proton affinity of pyridine (PA(pyridine) = 928.8 ± 0.9 kJ/mol) from a measurement of the proton transfer equilibrium constant at variable temperature.[24] Retaining this value in Table 1, the calculated "isodesmic" proton affinity of pyrimidine and 2-aminopyridine at the B3LYP/6-31+G(d,p)//B3LYP/6-31+G(d,p) and B3LYP/6-311++G(3df,2p)//B3LYP/6-31+G(d,p) levels agree within ca. 2 kJ/mol with their tabulated experimental values[8] (885.8 and 947.2 kJ/mol for pyrimidine and 2-aminopyridine, respectively). Note that the isodesmic correction also remove most of the discrepancies observed with the B3LYP/6-31G(d,p)//B3LYP/6-31G(d,p) data.

As detailed in the Supporting Information S1, the experimental range of PA(adenine) is 939−942 kJ/mol. It was of obvious interest to see as to whether our isodesmic procedure is able to reproduce the experimental data. The gas phase protonation of isolated adenine is predicted by theory to occur preferentially at N1 and N3 (Scheme 1A).[14] At all levels of theory very similar proton affinities are calculated for the two positions although the N1 position is slightly preferred over N3. According to CCSD(T)/6-311++G(3df,2p) calculations,[14e] the highest theoretical level used so far, the PAs of N1 and N3 are equal to 939 and 932 kJ/mol, respectively. The other basic sites are N7 (PA = 904 kJ/mol) and N10 (PA = 850 kJ/mol); the carbon atoms have PAs lower than 750 kJ/mol. The proton affinity of N1 predicted by our isodesmic procedure at the B3LYP/6-311++G(3df,2p)//B3LYP/6-31+G(d,p) level is equal to 941 kJ/mol and is consequently in excellent agreement with computations performed via coupled-cluster theory,[14e] post-Hartree−Fock MP4 method[14d] and with experiments in Table 1. Another important finding is that the relative energies of the protonated adenine tautomers N3 and N7 are predicted to be ∼7 and ∼35 kJ/mol above N1 (Table 2), independent of the method (DFT or post Hartree−Fock) and the presence of diffuse functions in the basis set.

TABLE 2: Relative 298 K Enthalpies of the Protonated Adenine Tautomers (kJ/mol)

	N1	N3	N7	reference
6-31G(d,p)[a]	0	6.3	34.9	
6-31+G(d,p)[a]	0	6.3	33.9	
6-311++G(3df,2p)[b]	0	5.2	33.2	
MP2/6-311+G(2d,2p)// MP2/6-31G(d)	0	8.3	37	14c
B3-MP2/6-311+G(3df,2p)	0	7	34	14e

[a] Geometry optimized and vibrational contribution calculated at this level. [b] On 6-31G(d,p) optimized geometries.

Simple Kinetic Method versus Extended Kinetic Method. For both the simple and the extended kinetic methods,[11] the idea is to study competitive dissociation of proton bound dimers between a series of reference compounds, B_i, and the compound of interest, M:

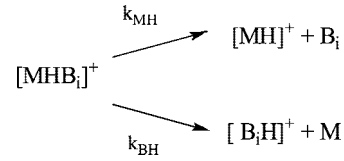

According to absolute rate theory and to assumptions that (i) transition state structures of each dissociation channel are close to the corresponding final states in structure and in energy and, (ii) the ratio of peak intensities between the $[MH]^+$ and $[BH]^+$ ions are equal to the ratio of the rate constants k_{MH}/k_{BH}, the natural logarithm of the peak ratio can be expressed by

$$y = \ln(k_{MH}/k_{BH}) = \ln([MH]^+/[BH]^+) = [G_T°(M) + G_T°(BH^+) - G_T°(MH^+) - G_T°(B)]/RT \quad (1)$$

where $G°$s are individual Gibbs free energies and T is an "effective temperature" related to the excitation energy of the dissociating $[MHB]^+$ species.[25] By introducing the gas phase basicities, GB, or proton affinities, PA, at 298 K in eq 1, y may also be written:

$$y = [GB_{298}(M) - GB_{298}(B) + (T - 298)\Delta_{MB}S°_{298} + \Delta H°_{298\rightarrow T} + T\Delta S°_{298\rightarrow T}]/RT \quad (2)$$

$$y = [PA_{298}(M) - PA_{298}(B) + T\Delta_{MB}S°_{298} + \Delta H°_{298\_T} + T\Delta S°_{298\_T}]/RT \quad (3)$$

where $\Delta_{MB}S°_{298} = S°_{298}(MH^+) + S°_{298}(B) - S°_{298}(M) - S°_{298}(BH^+) = \Delta_p S°_{298}(M) - \Delta_p S°_{298}(B_i)$.

As $MH^+ + B_i$ and $M + B_iH^+$ show clear structural similarity, we can assume that the terms $\Delta H°_{298\rightarrow T}$ and $\Delta S°_{298\rightarrow T}$, corre-

sponding to thermal corrections for enthalpy and entropy, are negligible.[11,25,26] In this case, eqs 2 and 3 can be reduced to:

$$y = [GB_{298}(M) - GB_{298}(B) + (T - 298)\Delta_{MB}S]/RT \quad (4)$$

$$y = [PA_{298}(M) - PA_{298}(B) + T\Delta_{MB}S]/RT \quad (5)$$

at the effective temperature T.

The simple kinetic method consists in measuring the y value for different couples of reference compounds B_i and the compound of interest M at a fixed effective temperature T, i.e., at fixed excitation energy. In other words, dissociation spectra of the proton bond dimer [MHB]+ must be collected at a fixed E_{cm} value. By plotting y versus $PA_{298}(B_i)$, or $GB_{298}(B_i)$, the thermochemical parameter $PA_{298}(M)$, or $GB_{298}(M)$, can be easily deduced if $\Delta_{MB}S$ is known or negligible. Obviously, when the term $\Delta_{MB}S$ is not negligible, the simple kinetic method is inappropriate since the x-intercept of the line y vs $PA_{298}(B_i)$ (see eq 5) is equal to an apparent proton affinity related to the proton affinity at 298 K (PA_{298}) by

$$PA_{app}(M) = PA_{298}(M) + T\Delta_{MB}S \quad (6)$$

In order to overcome this entropy problem, the extended kinetic method has recently been developed.[11] It consists of acquiring CID spectra of the proton bond dimer $[MHB]^+$ for various E_{cm} values, allowing for a variation of the effective temperature T, and to deduce the thermochemical parameters, $GB_{298}(M)$, $PA_{298}(M)$ and $\Delta_pS°_{298}(M)$. In this case, y_{ij} values are calculated for n_j different activation energy values and n_i different bases B_i.[11e−h,j] Then, the y_{ij} versus $PA_{298}(B_i)$ points are fitted by a set of regression lines $(y_{ij})_{calc} = y_0 + b_j(x_0 - x_i)$ intersecting in a common point at coordinate $x_0 = PA_{iso}(M)$ and $y_0 = \Delta S°_{iso}/R$, the so-called "isothermal"[11j] or "isoequilibrium"[11h] point. The precise coordinates can be localized by a statistical treatment, which simultaneously takes into account all the $[n_i,n_j]$ data points. A method, based on a least-squares regression analysis, called "orthogonal distance regression" (ODR) analysis has been used in the present work to deduce $PA_{iso}(M)$ and $\Delta_{MB}S°_{iso}/R$ from the experimental data points.[11h,16] In theory, $PA_{iso}(M)$ and $\Delta S°_{iso}$ should be equal to $PA_{298}(M)$ and to the mean value of the entropy terms $\langle\Delta_{MB}S°\rangle$, respectively. Alternatively, using the variable $y' = y - \Delta_pS°_{298}(B_i)/R$, would directly lead to $\Delta_pS°_{298}(M)$ from the y' coordinate of the isothermal point.

It has recently been observed that $PA_{iso}(M)$ and $\Delta S°_{iso}$ determined by the extended kinetic method would present systematic errors apparently linked to the size of the protonation entropies.[11g−i] Experimental results obtained on a large set of bi- or tridentate bases have confirmed these systematic deviations.[11j] The main implication of these studies is that the proton affinity PA(M) and of the absolute value of $\Delta_pS°(M)$ are underestimated when using the extended kinetic method. These systematic errors are however negligible when $\Delta_pS°(M)$ is less than ca. 10 $J\cdot mol^{-1}\cdot K^{-1}$. Moreover, and whatever the size of $\Delta_pS°(M)$, it has been demonstrated that the corresponding gas phase basicity GB(M) is correctly estimated by the isothermal extended kinetic method. In fact, when compiling 35 experiments based on the extended kinetic method, a mean deviation of only 2.4 $kJ\cdot mol^{-1}$ has been reported between $GB_{iso}(M) = PA_{iso}(M) - 298\ (S°_{298}(H^+) - \Delta_pS°_{iso})$ and the values reported in the NIST database.[11j]

Experimental Determination of the Gas-Phase Protonation Thermochemistry of Adenosine. Adenosine and four reference bases, namely dinpropylamine, di-isopropylamine, triethylamine and tri-*n*-propylamine, have been used to produce MHB_i+ ions by nanoESI source. As described in the Experimental and Computational Methods, the $[MH]^+$ and $[B_iH]+$ intensities were obtained by summing the intact and fragment ion abundances of each protonated species. In Figure 1, the ions at m/z 268 and m/z 102 correspond to the protonated adenosine and dinpropylamine, respectively. The ion at m/z 136 corresponds to protonated adenine and arises from the loss of the ribose moiety from protonated adenosine.[27] The breakdown curves of the ion at m/z 268 (Figure 2) clearly show that the fragment at m/z 136 must absolutely be taken into account for the determination of the [MH]+ intensity, specially when E_{cm} is higher than 1 eV.

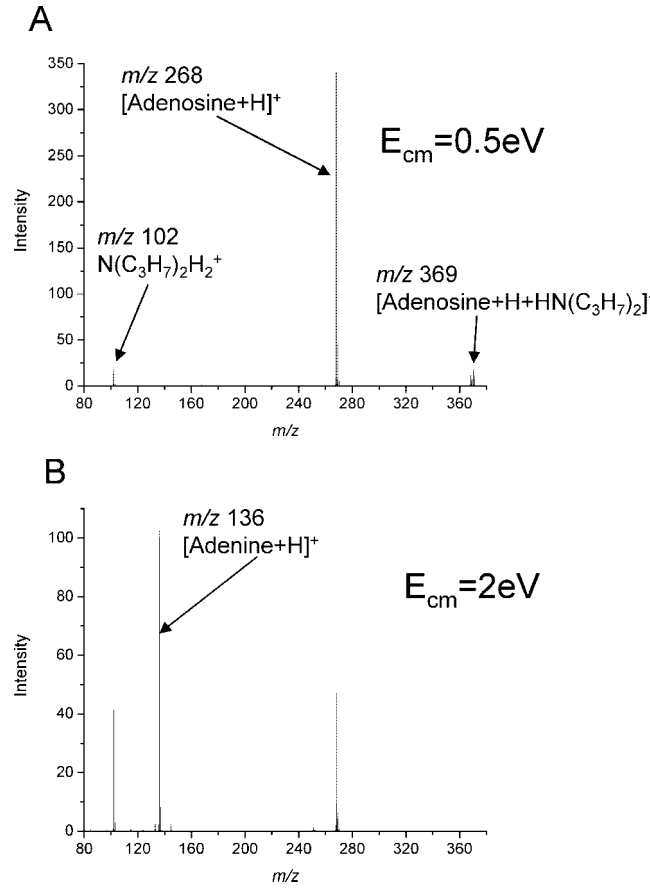

Figure 1. Mass spectrum of the proton-bond dimer [adenosine + H + di-*n*-propylamine]+ and its dissociation products for $E_{cm} = 0.5$ eV (A) and 2 eV (B).

The isothermal point was determined using $\ln([MH]^+/[BH]^+)$ at fixed E_{cm}, extrapolated from the data obtained at fixed $E_{laboratory}$ (Figure 2 in Supporting Information). Figure 3 illustrates the ODR treatment of the total set of 16 data points using the variable y. A similar figure (not represented) is obtained using y' as variable. Combining y and y' results, PA_{iso} and $\Delta_pS°_{iso}$ for adenosine were determined to be 979.2 ± 1.1(2.3) kJ/mol and −5 ± 5(8) J/mol·K, respectively (indicated errors are standard deviation and, into parentheses, 95% confidence limits), and consequently GB_{298}(adenosine) = 945.3 ± 1.9(3.3) kJ/mol.

In 1994, Liguori et al. performed PA_{app} measurement for adenosine using the simple kinetic method, obtaining a value of 974.3 kJ/mol.[11c] This value was corrected to 989.4 kJ/mol by the authors themselves in 2000 using the presently accepted PA for the reference bases.[10a] The GB(adenosine) value reported in the NIST database (956.8 kJ/mol) was simply extrapolated from the Liguori et al.[10a,c] data using the approximation of a zero-entropy protonation reaction.[8] A difference of ca. 10 kJ/

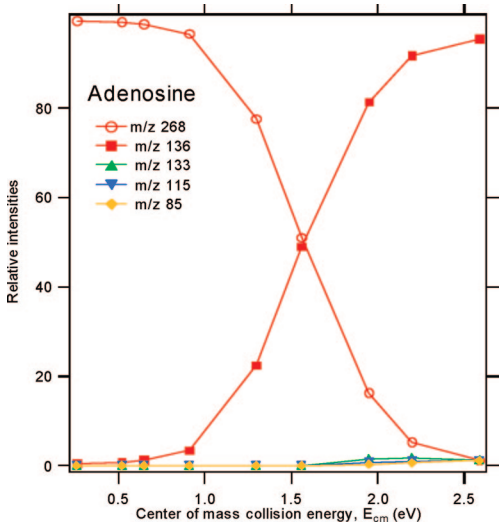

Figure 2. Breakdown curve of the protonated adenosine obtained by plotting the relative intensities of the precursor ion (*m/z* 268) and the fragment ion (*m/z* 136) versus E_{cm}.

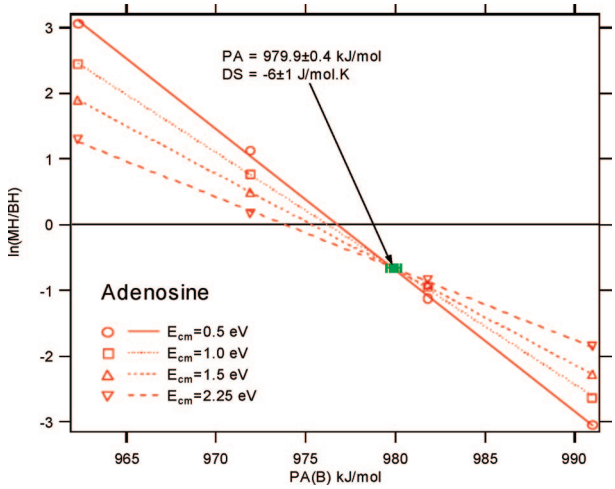

Figure 3. Kinetic method plot *y* vs PA(B_i) obtained for four center-of-mass collision energies (E_{coll}). The isothermal point was determined by the ODR method.

mol for both AP and GB is observed between our measurements and Liguori. The origin of this discrepancy is not clear. It may be noted that different ionization techniques (nanoESI versus FAB), activation processes (CID versus MIKE) and observation time windows (ms versus μs) were used, this is not expected however to alter a comparison since all these experimental parameters are supposed to be accounted for in the effective temperature *T*.[10] Another remark is that Liguori et al.[10c] used relative abundances of the fragment ions "corrected for the discrimination effect of the electron multiplier". The authors do not explain however as to what this correction consists of, which has the net consequence of shifting by ca. 2.5 logarithm units the *y* values as observed by the comparison with our data obtained with the same reference bases triethylamine and tripropylamine.

Nevertheless, none of the MS experiments could actually answer the following questions: Where is the proton attached? What is (are) the most stable conformation(s) of protonated adenosine? Why is such a small entropy loss observed upon protonation? Only a careful theoretical investigation of the protonation of isolated adenosine can provide suitable information, as will be examined in the following section.

SCHEME 2: Two Examples of Twist Conformers for a Furanose Ring

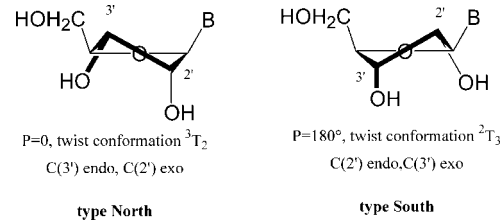

SCHEME 3: Pseudo-Rotation Wheel and Corresponding Nomenclature for Furanose Rings

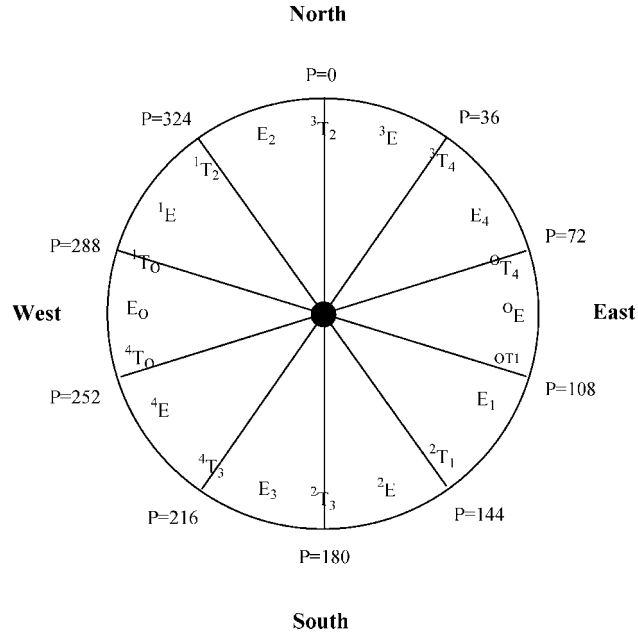

Conformational Analysis of Neutral Adenosine. In order to calculate the proton affinity of adenosine (Scheme 1B) it is obviously necessary to identify the most stable conformations of its neutral and protonated forms. Conformational analysis of adenosine may be separated into several, not completely independent, problems: (i) the search for the most stable conformers of the flexible furanose ring, (ii) the dramatic influence of the mutual orientation of the adenine moiety and the furanose part, (iii) consideration of the $C_{4'}$-$C_{5'}$ rotamers, and, finally, (iv) the role of the various possible internal hydrogen bonds.

The furanose ring presents ten possible envelope conformations denoted E and characterized by the "endo" (^{i}E) or "exo" (E_i) position of the out-of-plane atom i. The passage from one envelope to its nearest homologue is assumed by a twisted form $^{i}T_j$ (Scheme 2).

This conformational change has been already described in terms of pseudorotation by defining a phase angle P as a general variable including the various dihedral angles of the cycle.[28] A complete pseudorotational cycle is described between $P = 0$ and $P = 360°$ allowing the alternative passage trough the ten envelopes (E) and the 10 twisted (T) conformers (Scheme 3). The various conformers are termed either north or south depending upon their location in the pseudorotation wheel (two examples of twist conformers are presented in scheme 2). From X-ray studies it is well-known that nucleotides fall into two ranges of furanose ring conformers denoted C(2′)-endo or south and C(3′)-endo or north. Moreover, consideration of a large number of experimental data shows that nucleotides fall into

SCHEME 4: Definition of the Three Possible Rotamers about the $C_{4'}-C_{5'}$ Bond

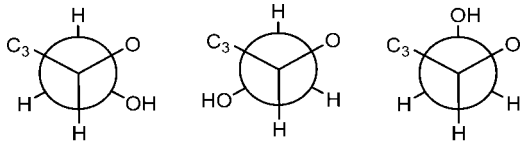

SCHEME 5: The Two Types of O(3′)HO(2′) Interactions

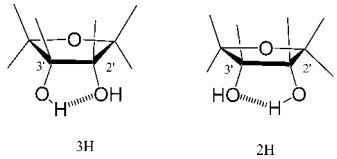

two very narrow pseudorotational angle ranges, mainly represented by envelopes ^{3}E (north) and ^{2}E (south). Adenosine and adenosine 5′-phosphate, in particular, appear to be more stable in their ^{3}E north conformation in condensed phase.[28]

A recent theoretical study of model compounds confirms this general trend, though contrasting situations are revealed.[29] For example, the preferred conformation of isolated methyl β-D-ribofuranose is calculated to be ^{4}E, E$_3$, and ^{2}E, all pertaining to the south class. As it will be seen below, in the present computational study, most of energy minima located for adenosine are related to the ^{2}E (i.e., C(2′)-endo or south) conformation type. This general trend is the result of several favorable interactions involving not only the floppy character of the furanose ring but also the orientation about the $C_{4'}-C_{5'}$ bond and the possibilities of intramolecular hydrogen bonds involving the 2′, 3′ and 5′ hydroxyl groups. Schemes 4 and 5 present the nomenclature used to name these various conformational characteristics. Rotation around the $C_{4'}-C_{5'}$ bond leads to three possible conformers: "gauche−trans" (gt), "trans−gauche" (tg) and "gauche−gauche" (gg) (Scheme 4). As a rule, the gg conformer is found to be the lowest in energy because it allows stabilizing interactions between the hydroxyl group and one atom of either the ribose or the adenine moieties.

Concerning the intramolecular hydrogen bonds involving the 2′ and 3′ hydroxyl groups, their orientations depend upon the North or South character of the ribose part and on the nature of the possible interaction of O(2′)H with the adenine heterocycle. "3H" will be the arrangement allowing a O(3′)H···O(2′) hydrogen bonding and "2H" the reverse situation, O(3′)···HO(2′) (Scheme 5).

Finally we investigate the conformational space by rotating both, adenine and ribose, subsystems around the C(1′)-N(9) bond. The related potential energy profile is presented in Figure 4 and the total energies of the various local minima are indicated in Table 3 (see also Supporting Information in Table S2). Figure 4 clearly shows three minima in the potential energy versus HC(1′)N(9)C(4) dihedral angle curve. It corresponds to the three ^{2}E (south) most stable conformers of adenosine identified in the present study at the B3LYP/6-31G(d,p) level. Their HC(1′)N(9)C(4) dihedral angles are equal to −175.9°, −75.4°, and 4.9° and, for this reason, they are called $S_{3H(180)}$, $S_{3H(90)}$, and $S_{3H(0)}$, respectively (Figure 4).

The two conformers $S_{3H(180)}$ and $S_{3H(90)}$ are of comparable stabilities, their relative energies fall in a very narrow range of 3 kJ/mol at the three levels of theory used here (Table 3). The conformer $S_{3H(90)}$ is characterized by a noticeable hydrogen bond involving the H atom of the OH(2′) hydroxyl group and the

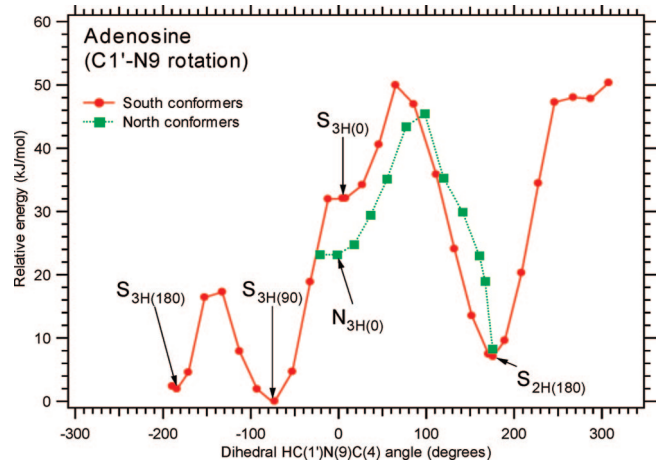

Figure 4. B3LYP/6-31G(d,p) potential energy profile associated to rotation around the C(1′)N(9) bond.

TABLE 3: Relative 298 K Enthalpies, $\Delta H°_{298}$ of Neutral Adenosine Conformers (kJ/mol)

M	conformer	method[a]	ΔH_{298}
adenosine	$S_{3H(180)}$	A	2
		B	0
		C	0
	$S_{3H(90)}$	A	0
		B	0
		C	3
	$S_{3H(0)}$	A	31
	$S_{2H(180)}$	A	7
		B	7

[a] Method: A = B3LYP/6-31G(d,p)//B3LYP/6-31G(d,p), B3LYP/6-31G(d,p) vibrational contribution; B = B3LYP/6-31+G(d,p)// B3LYP/6-31+G(d,p), B3LYP/6-31+G(d,p) vibrational contribution; C = B3LYP/6-31++G(3df,2p)// B3LYP/6-31G(d,p), B3LYP/6-31+G(d,p) vibrational contribution.

nitrogen N(3) (d = 1.883 Å, Figure 5). Conformer $S_{3H(180)}$ also forms a hydrogen bond which again involves the nitrogen atom N(3) but with the acidic hydrogen of the OH(5′) (d = 1.897 Å, Figure 5). Note that structure $S_{3H(0)}$ is only marginally stable, it is situated 32 kJ/mol above $S_{3H(90)}$ and may easily collapse to the latter (see Figure 4). In fact, no particular stabilizing interaction exists between adenine and the hydroxyl groups of the ribose moiety in conformer $S_{3H(0)}$. Moreover, when increasing the HC(1′)N(9)C(4) dihedral angle above 30° it turns out that a repulsive interaction between H(8) and the hydroxylic hydrogen of OH(2′) forces the latter to rotate and thus to pass into the S_{2H} part of the conformational space and to produce the $S_{2H(180)}$ conformer. The barrier $S_{3H(90)} \rightarrow S_{2H(180)}$ (ca. 50 kJ/mol) thus corresponds mostly to the 3H → 2H change of hydrogen bonding character (Scheme 5). Note that the passage $S_{3H(180)} \rightarrow S_{3H(90)}$, which involves breaking of the hydrogen bond O(5′)H···N(3) is less energy demanding since it needs only 18 kJ/mol.

Examination of the north conformers reveals the existence of structure $N_{3H(0)}$ situated 23 kJ/mol above $S_{3H(90)}$ and more stable than $S_{3H(0)}$ by 9 kJ/mol. This conformer, like its congener $S_{3H(0)}$, is however in a very shallow potential energy well and should be considered metastable. It is interesting to note that for HC(1)N(9)C(4) dihedral angles values lower than −20° and larger than +180°, all tentative of optimization of the north conformer collapse to the corresponding south counterpart.

In summary, isolated adenosine presents essentially three stable conformations, $S_{3H(180)}$, $S_{3H(90)}$ and $S_{2H(180)}$, separated by

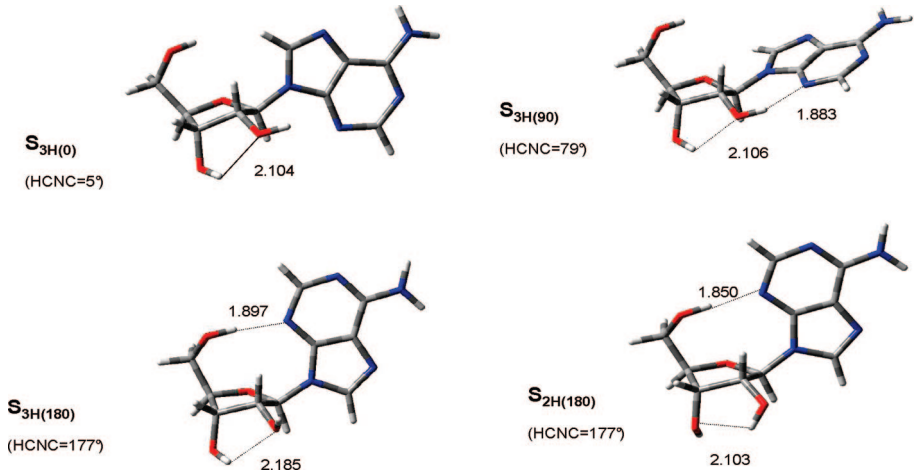

Figure 5. Optimized B3LYP/6-31+G(d,p) geometries of the most stable conformers of adenosine.

TABLE 4: Relative 298 K Enthalpies, $\Delta H°_{298}$ of Protonated Adenosine Conformers and Corresponding Proton Affinities (kJ/mol)

M	conformer	method[a]	ΔH_{298}	$PA_{isodesmic}$[b]
adenosineH$^+$ (N1 protonated)	$S_{3H(180)}$N1	A	44	
	$S_{3H(90)}$N1	A	51	
	$S_{3H(0)}$N1	A	33	
	$S_{2H(180)}$N1	A	50	
adenosineH$^+$ (N3 protonated)	$S_{3H(180)}$N3	A	0	978.2
		B	0	971.9
		C	0	973.6
	$S_{3H(90)}$N3	A	22	955.7
	$S_{2H(180)}$N3	A	10	968.5
		B	11	
	$S_{2H(90)}$N3	A	3	975.0
		B	3	968.4
		C	4	969.9
adenosineH$^+$ (N7 protonated)	$S_{3H(180)}$N7	A	62	
	$S_{3H(90)}$N7	A	43	
	$S_{3H(0)}$N7	A	51	
	$S_{2H(180)}$N7	A	54	

[a] Method: A = B3LYP/6-31G(d,p)// B3LYP/6-31G(d,p), B3LYP/6-31G(d,p) vibrational contribution; B = B3LYP/6-31+G(d,p)// B3LYP/6-31+G(d,p), B3LYP/6-31+G(d,p) vibrational contribution; C = B3LYP/6-31++G(3df,2p)// B3LYP/6-31G(d,p), B3LYP/6-31+G(d,p) vibrational contribution. [b] Isodesmic 298 K proton affinities calculated with reference to PA(pyridine) = 928.8 kJ/mol.

significant energy barriers (18 and 50 kJ/mol, Figure 4). At all levels of theory used here, conformers $S_{3H(180)}$ and $S_{3H(90)}$ are predicted to be of comparable stabilities, which should be borne in mind when looking at the protonation thermochemistry of adenosine.

Protonation Sites of Adenosine. Protonation of adenosine on the three nitrogen atoms N(1), N(3), and N(7) was investigated at the B3LYP/6-31G(d,p) level of theory. For each possible protonation site, a complete rotational scan around the C(1′)N(9) bond was performed. A total of twelve local minima were located, whose total energies are reported in Table 4. As a rule, protonated adenine conformers exhibit weakened hydrogen bonds between the hydrogen of either the 5′ or the 2′ hydroxyl group and the adenine heterocycle due to the location of the positive center on this latter. Moreover, the most stable protonated adenine conformers generally exhibit a new hydrogen bond pointing in the reverse direction, i.e., the acidic hydrogen is located in the protonated heterocyclic part and the hydrogen acceptor is an oxygen atom of the ribose moiety.

Protonation on N1, the most basic site of isolated adenine (see above), leads to four south conformers, $S_{3H(0)}$N1, $S_{3H(90)}$N1, $S_{3H(180)}$N1 and $S_{2H(180)}$N1. These structures are probably only marginally stabilized by intramolecular hydrogen bonds. Accordingly, with respect to their neutral counterparts, the protonated conformers $S_{3H(90)}$N1, $S_{3H(180)}$N1 and $S_{2H(180)}$N1 show elongated hydrogen bond distances. The O(5′)H···N3 distance is equal to 2.077 Å and 2.055 Å (Figure 6) in $S_{3H(180)}$N1 and $S_{2H(180)}$N1, while it amounts to 1.897 Å and 1.850 Å for $S_{3H(180)}$ and $S_{2H(180)}$, respectively. Similarly, the O(2′)H···N3 distance goes from 1.883 Å in $S_{3H(90)}$ to 2.132 Å in $S_{3H(90)}$N1. The most stable form, $S_{3H(0)}$N1, possesses a favorable interaction between C(8)H and O(5′) which was absent in $S_{3H(0)}$, however the large distance observed between the interacting atoms (d = 2.309 Å, Figure 6) results in only one contribution of this interaction to the internal stabilization of this conformer. The reason for the largest stability of $S_{3H(0)}$N1 with respect to the other N1 protonated forms probably lies on more global effects such as dipole−dipole and dipole-polarizable interactions.

The major finding here is that, due to the weakness of their internal electrostatic interactions, the four N1 protonated conformers do not constitute the most probable protonated forms of adenosine. As can be seen from examination of Table 4 (see also Supporting Information in Table S2), structures $S_{3H(0)}$N1, $S_{3H(90)}$N1, $S_{3H(180)}$N1 and $S_{2H(180)}$N1 are situated 30 to 50 kJ/mol above the N3 protonated adenosine conformers. This result is clearly at variance with N1 being the most probable protonation site of the adenine molecule.

Protonation on N3 is predicted to produce four stable South conformers, two of 3H type $S_{3H(90)}$N3, $S_{3H(180)}$N3 and two of 2H type, $S_{2H(90)}$N3 and $S_{2H(180)}$N3 (Figure 7). The three most stable conformers draw their stability from a strong hydrogen bond appearing between N(3)H and either O(5′), $S_{3H(180)}$N3 (d = 1.812 Å, Figure 7) and $S_{2H(180)}$N3 (d = 1.823 Å, Figure 7), or O(2′), $S_{2H(90)}$N3 (d = 1.865 Å, Figure 7). Note that a similar bonding is expected in conformer $S_{3H(90)}$N3 between N(3)H and O(2′), however an optimum arrangement is limited due to the existence of the 3H type O(3′)H···O(2′), interaction.

The two most stable conformers $S_{3H(180)}$N3 and $S_{2H(90)}$N3 are very close in energy (within less than 3 kJ/mol) and their formation should be considered as equally probable. Starting from $S_{3H(180)}$N3, a rotation around the C(1)−N(9) bond leads to conformer $S_{2H(90)}$N3. Inversion of the hydrogen bonding 3H/2H follows the rotation in order to accommodate the N(3)H···O(2′) hydrogen bonding in $S_{2H(90)}$N3. The calculated energy barrier associated with this transformation is ca. 50 kJ/mol. A rotation around the C(1)−N(9) bond allows the passage from conformer $S_{2H(90)}$N3 to $S_{2H(180)}$N3, the corresponding energy barrier

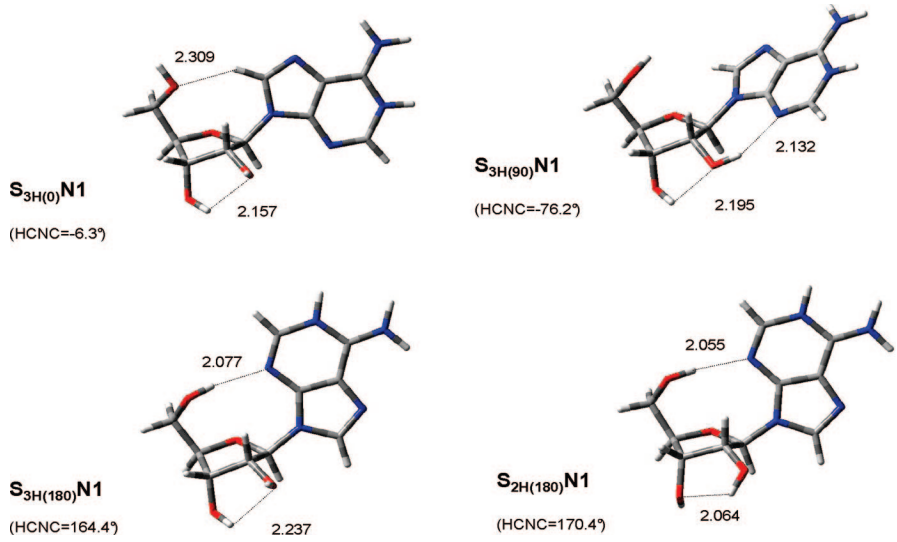

Figure 6. Optimized B3LYP/6-31G(d,p) geometries of the most stable conformers of adenosine protonated on N1.

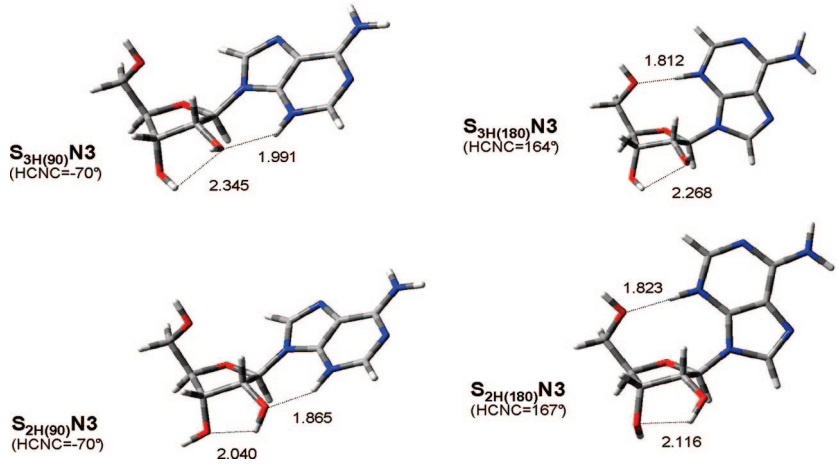

Figure 7. Optimized B3LYP/6-31+G(d,p) geometries of the most stable conformers of adenosine protonated on N3.

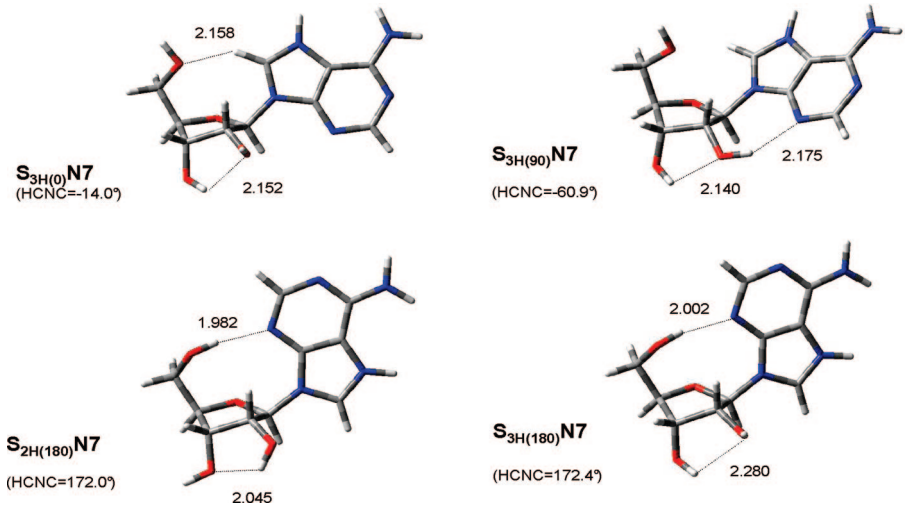

Figure 8. Optimized B3LYP/6-31G(d,p) geometries of the most stable conformers of adenosine protonated on N7.

calculated at the B3LYP/6-31+G(d,p) level, is situated 36 kJ/mol above $S_{2H(90)}N3$.

Protonation on N7 leads to structures of high energies, situated 40−60 kJ/mol above the N3 protonated adenosine conformers, which are thus unlikely to be produced in our experimental conditions. Four conformers have been identified, $S_{3H(0)}N7$, $S_{3H(90)}N7$, $S_{3H(180)}N7$, and $S_{2H(180)}N7$ (Figure 8). Two reasons place these structures well above the minimum $S_{3H(180)}N3$. First, N7 is the least basic of the three investigated nitrogen atoms of the heterocyclic adenine part. Second, no favorable intramolecular hydrogen bonding is operating in these various conformers. Moreover, the OH···N3 hydrogen bonds that exists in the neutral precursors are weakened in the protonated forms. This is illustrated by the OH···N3 distances which become equal to

TABLE 5: Calculated B3LYP 298 K Proton Affinities of Adenosine (in kJ/mol)

	pyridine	adenosine ($S_{3H(180)}N_3$)	adenosine ($S_{2H(90)}N_3$)
6-31G(d,p)[a]	954.4	1003.8	1000.6
6-31+G(d,p)[a]	936.0	979.1	975.6
6-311++G(3df,2p)[b]	936.7	981.5	977.8
experiment[c]	928.8	979.9	
iso6-31G(d,p)[d]	928.8	978.2	975.0
iso6-31+G(d,p)[d]	928.8	971.9	968.4
iso6-311++G(3df,2p)[d]	928.8	973.6	969.9

[a] Geometry optimized and vibrational contribution calculated at this level. [b] On B3LYP/6-31G(d,p) optimized geometries. [c] See text for the relevant literature and comments. [d] Isodesmic 298 K proton affinities calculated with reference to PA(pyridine) = 928.8 kJ/mol.

2.175 Å, 1.982 Å and 2.002 Å in $S_{3H(90)}N7$, $S_{3H(180)}N7$, and $S_{2H(180)}N7$ (Figure 8), respectively, but were shorter in the corresponding neutrals.

There is no doubt that protonation of adenosine should occur on the N(3) position, since there is no competition from either N(1) or N(7). This finding differs from the adenine and apparently also from 2′-deoxyriboadenosine[15] where the N(1) position is the most basic site. In this regard, the formation of intramolecular hydrogen bonds involving N(3)H and either O(5′) or O(2′), in conformers $S_{3H(180)}N3$ and $S_{2H(90)}N3$ is crucial for the stabilization of protonated adenosine.

Theoretical Protonation Thermochemistry. Computed proton affinities (isodesmic B3LYP/6-31+g(d,p) 298 K enthalpies) of adenosine are summarized in Table 5 (see also Supporting Information in Table S2). The most favorable protonation process involves conformers $S_{2H(90)}N3$ and $S_{3H(180)}N3$, and the corresponding calculated proton affinity is equal to 974 kJ/mol at the B3LYP/6-31++G(3df,2p)//B3LYP/6-31G(d,p) level including the isodesmic correction described above. This value compares favorably with our experimental determination of 979 ± 1 kJ/mol. A correction of the proton affinity based on the population of neutral and protonated adenosine is not expected to change the PA estimate based on one neutral and one protonated conformer. Moreover, the difference of 3 kJ/mol in PA $S_{3H(180)}N3$ and $S_{2H(90)}N3$ in Table 5 is probably less than the calculations uncertainty.

A major observation is that comparable entropies are expected for both neutral and protonated adenosine. Accordingly, only two conformers are expected to essentially represent the population of neutral ($S_{3H(180)}$ and $S_{3H(90)}$) and protonated ($S_{3H(180)}N3$ and $S_{2H(90)}N3$) adenosine. The first consequence is that no difference in entropy of mixing between the neutral and protonated species is expected. The second point is that neutral and protonated conformers are separated by a significant energy barrier along the C−N rotation (18 kJ/mol for the neutral and 36 kJ/mol for the protonated forms). The change in entropy due to the change in rotational barrier may be approximated by considering the Pitzer and Gwinn tables of thermodynamic functions for molecules with internal rotation.[30] Following these data, the increase in rotational barrier from 18 to 36 kJ/mol should be associated with a maximum decrease in entropy of -3.3 J·mol^{-1}·K^{-1} at 298 K. This may be considered as an estimate of the protonation entropy of adenosine. It is noteworthy that the rotational are high enough to allow the use of the harmonic oscillator approximation in the description of the hindered rotation. Under these circumstances, the entropy values given by Gaussian, which are based on the harmonic oscillator approximation may be used in order to estimate the $\Delta_p S°$(adenosine). The $S°$ values calculated at the B3LYP/6-31+G(d,p) level are 128.6, 131.1, 127.8 and 130.0 J·mol^{-1}.K^{-1} for $S_{3H(180)}$, $S_{3H(90)}$, $S_{3H(180)}N3$, and $S_{2H(0)}N3$, respectively. These figures lead to a protonation entropy of −1.8 J/mol·K. Consequently, theoretical arguments converge on a protonation entropy of adenosine sligthly negative, of $-3/-2$ J·mol^{-1}·K^{-1}, in agreement with the experimental estimate of -5 ± 5 J·mol^{-1}·K^{-1} given by the extended kinetic method.

IV. Conclusion

Three major conclusions on the gas-phase protonation thermochemistry of adenosine can be drawn from our experimental and theoretical studies:

(1) We determined a proton affinity of 979 ± 1 kJ/mol for gas-phase adenosine, by the extended kinetic method using nanoESI-CID-MS/MS. This value agrees well with the one obtained by DFT calculations at the B3LYP/6-311++G(3df,2p)//B3LYP/6-31+G(d,p) level and using an isodesmic procedure (974 kJ/mol). A difference of ∼10 kJ/mol is observed between our measurements and the earlier ones based on a FAB-MIKE-MS/MS experiment.[9] This should result in a correction of the values in the NIST database, which are frequently used by all chemists as reference values.

(2) Theoretical studies are of great value for locating the protonation site and understanding the conformational changes during protonation. The present calculations showed clearly that the N3 position is the most favorable site of protonation, in contrast with adenine and deoxyadenosine, where N1 is the most basic site. This is due to the strong hydrogen bond interactions occurring between one oxygen atom of the sugar and the added proton in the N3 position of the base.

(3) The protonation entropy of adenosine is negligible or slightly negative as established from experiment ($\Delta_p S°$(adenosine) = −5 ± 5 J/mol·K), and also predicted by theory (−2/−3 J/mol·K). This entropy contribution combined with the proton affinity determination allow the gas-phase basicity of adenosine to be evaluated to GB(adenosine) = 945 ± 2 kJ/mol.

The present study demonstrates once again that a joint approach, using up of date experimental and theoretical methods, is essential in the understanding of gas phase protonation processes. From this point of view, the protonation thermochemical properties of nucleosides that were formerly measured may be reconsidered and extended to mono- and polynucleotides, for which very little data is currently available.[31]

Acknowledgment. We thank the Novartis Institutes for BioMedical Research for financial support and Professors Kent Ervin and Peter Armentrout for providing us with the ODR program.

Supporting Information Available: Text giving a retreatment of the data published by Greco *at al*. for adenine and a figure giving a plot of the kinetic method (section S1), a figure showing the evolution of ln(MH/B_iH) as a function of the center of mass collision energy E_{cm} for adenosine and 4 different reference bases (section S2), and tables of computed geometrical parameters, total energies, 298K correction to enthalpies, 298 K enthalpies (in Hartree) and proton affinities (in kJ/mol) for pyridine, pyrimidine, 2-aminopyridine, adenine and adenosine (section S3). This material is available free of charge via the Internet at http://pubs.acs.org.

References and Notes

(1) (a) Watson, J.; Crick, F. *Nature* **1953**, *171*, 737–738. (b) Ponnuswamy, P.; Gromiha, M. *J. Theor. Biol.* **1994**, *169*, 419–432.

(2) Knowles, J. R. *Annu. Rev. Biochem.* **1990**, *49*, 877–919.
(3) Dodge-Kafka, K. L.; Kapiloff, M. S. *Eur. J. Cell Biol* **2006**, *85*, 593–602.
(4) Belenky, P.; Bogan, K. L.; Brenner, C. *Trends Biochem. Sci.* **2007**, *32*, 12–19.
(5) Tu, B. P.; Weissman, J. S. *J. Cell Biol.* **2004**, *164*, 341–346.
(6) Ganguly, S.; Kundu, K. K. *J. Solution Chem.* **1994**, *23*, 1227–1246.
(7) Wilson, M. S.; McCloskey, J. A. *J. Am. Chem. Soc.* **1975**, *97*, 3436–3444.
(8) Hunter, E. P.; Lias, S. G. *Standard reference database no. 69. NIST Chemistry Webbook*; National Institute of Standards and Technology: Gaithersburg, MD, 2005; http//webbook.nist.gov/chemistry/.
(9) Greco, F.; Liguori, A.; Sindona, G.; Uccella, N. *J. Am. Chem. Soc.* **1990**, *112*, 9092–9096.
(10) (a) Liguori, A.; Napoli, A.; Sindona, G. *J. Mass Spectrom.* **2000**, *35*, 139–144. (b) Di Donna, L.; Napoli, A.; Sindona, G.; Athanassopoulos, C. *J. Am. Soc. Mass Spectrom.* **2004**, *15*, 1080–1086. (c) Liguori, A.; Napoli, A.; Sindona, G. *Rapid Commun. Mass Spectrom.* **1994**, *8*, 89–93.
(11) (a) Cooks, R. G.; Kruger, T. L. *J. Am. Chem. Soc.* **1977**, *99*, 1279–1281. (b) Cooks, R. G.; Patrik, J. S.; Kotaho, T.; McLuckey, S. A. *Mass Spectrom. Rev.* **1994**, *13*, 287–339. (c) Cooks, R. G.; Wong, P. S. H. *Acc. Chem. Res.* **1998**, *31*, 379–386. (d) Cooks, R. G.; Koskinen, J. T.; Thomas, P. D. *J. Mass Spectrom.* **1999**, *34*, 85–92. (e) Bouchoux, G.; Djazi, F.; Gaillard, F.; Vierezet, D. *Int. J. Mass Spectrom.* **2003**, *227*, 479–496. (f) Bouchoux, G.; Buisson, D. A.; Bourcier, S.; Sablier, M. *Int. J. Mass Spectrom.* **2003**, *228*, 1035–1054. (g) Drahos, L.; Vekey, K. *J. Mass Spectrom.* **2003**, *38*, 1025–1042. (h) Ervin, K.; Armentrout, P. B. *J. Mass Spectrom.* **2004**, *39*, 1004–1015. (i) Drahos, L.; Peltz, C.; Vekey, K. *J. Mass Spectrom.* **2004**, *39*, 1016–1024. (j) Bouchoux, G. *J. Mass Spectrom.* **2006**, *41*, 1006–1013. (k) Bouchoux, G. *Mass Spectrom. Rev.* **2007**, *26*, 775–835.
(12) Mautner, M. *J. Am. Chem. Soc.* **1979**, *101*, 2396–2403.
(13) (a) Colson, A. O.; Besler, B.; Close, D. M.; Sevilla, M. D. *J. Phys. Chem.* **1992**, *96*, 661–668. (b) Colominas, C.; Luque, F. J.; Orozko, M. *J. Am. Chem. Soc.* **1996**, *118*, 6811–6821. (c) Russo, N.; Toscano, M.; Grand, A.; Jolibois, F. *J. Comput. Chem.* **1998**, *19*, 989–1000. (d) Ngyuen, M. T.; Chandra, A. K.; Zeegers-Huyskens, T. *J. Chem. Soc., Faraday Trans.* **1998**, *94*, 1277–1280. (e) Chandra, A. K.; Ngyuen, M. T.; Zeegers-Huyskens, T. *J. Phys. Chem. A* **1998**, *102*, 6010–6016. (f) Chandra, A. K.; Nguyen, M. T.; Uchimaru, T.; Zeegers-Huyskens, T. *J. Phys. Chem. A* **1999**, *103*, 8853–8060. (g) Podolyan, Y.; Gorb, L.; Leszcczynski, J. *J. Phys. Chem. A* **2000**, *104*, 7346–7352. (h) Moa, M. J. G.; Mandado, M.; Mosquera, R. A. *Chem. Phys. Lett.* **2006**, *428*, 255–261.
(14) (a) Russo, N.; Toscano, M.; Grand, A.; Jolibois, F. *J. Comput. Chem.* **1998**, *19*, 989–1000. (b) Chandra, A. K.; Nguyen, M. T.; Uchimaru, T.; Zeegers-Huyskens, T. *J. Phys. Chem. A* **1999**, *103*, 8853–8860. (c) Rodgers, M. T.; Armentrout, P. B. *J. Am. Chem. Soc.* **2000**, *122*, 8548–8558. (d) Podolyan, Y.; Gorb, L.; Leszczynski, J. *J. Phys. Chem. A* **2000**, *104*, 7346–7352. (e) Chen, X.; Syrstad, E. A.; Nguyen, M. T.; Gerbaux, P.; Turecek, F. *J. Phys. Chem. A* **2004**, *108*, 9283–9293.
(15) Xia, F.; Xie, H.; Cao, Z. *Int. J. Quantum Chem.* **2008**, *108*, 57–65.
(16) Boggs, P. T.; Byrd, R. H.; Rogers, J. E.; Schnabel, R. B. *ODRPACK Version 2.01 Software for weighted orthogonal distance regression; Report NISTIR 92−4834*; National Institute of Standards and Technology: Gaithersburg, MD, 1992.
(17) (a) *Gaussian 98, revision A.6*; Gaussian, Inc.: Pittsburgh, PA, 1998. (b) *Gaussian 03, revision B.04*; Gaussian Inc.: Pittsburgh, PA, 2003.
(18) (a) Hehre, W. J.; Ditchfield, R.; Radom, L.; Pople, J. A. *J. Am. Chem. Soc.* **1970**, *92*, 4796–4801. (b) Bouchoux, G.; Defaye, D.; McMahon, T. B.; Likholyot, A.; Mo, O.; Yanez, M. *Chem. Eur. J.* **2002**, *8*, 2900–2909.
(19) Sousa, S. F.; Fernandes, P. A.; Ramos, M. J. *J. Phys. Chem. A* **2007**, *111*, 10439–10452.
(20) Yao, C.; Turecek, F.; Polce, M. J.; Wesdemiotis, C. *Int. J. Mass Spectrom.* **2007**, *265*, 106–123.
(21) Curtiss, L. A.; Raghavachari, K.; Redfern, P. C.; Rassolov, V.; Pople, J. A. *J. Chem. Phys.* **1998**, *109*, 7764–7776.
(22) Baboul, A. G.; Curtis, L. A.; Redfern, P. C.; Raghavachari, K. *J. Chem. Phys.* **1999**, *110*, 7650–7657.
(23) Montgomery, J. A., Jr.; Frisch, M. J.; Ochterski, J. W.; Petersson, G. A. *J. Chem. Phys.* **2000**, *112*, 6532–6542.
(24) Meot-Ner (Mautner) , M.; Sieck, L. W. *J. Am. Chem. Soc.* **1991**, *113*, 4448–4460.
(25) Ervin, K. M. *Int. J. Mass Spectrom.* **2000**, *195/196*, 271–284.
(26) Bouchoux, G. *J. Phys. Chem. A* **2006**, *110*, 8259–8265.
(27) (a) Esmans, E. L.; Broes, D.; Hoes, I.; Lemiere, F.; Vanhoutte, K. *J. Chromatogr. A* **1998**, *794*, 109–127. (b) Di Donna, L.; Napoli, A.; Sindona, G. In *The Encyclopedia of Mass Spectrometry*; Gross, M. L., Capriomi, R. M., Eds.; Elsevier: Amsterdam, 2006; *Vol. 3*, pp 22−39.
(28) Altona, C.; Sundaralingam, M. *J. Am. Chem. Soc.* **1972**, *94*, 8205–8212.
(29) (a) Houseknecht, J. B.; Lowary, T. L.; Hadad, C. M. *J. Phys. Chem. A* **2003**, *107*, 372–378. (b) Houseknecht, J. B.; Lowary, T. L.; Hadad, C. M. *J. Phys. Chem. A* **2003**, *107*, 5763–5777.
(30) Pitzer, K. S.; Gwinn, W. D. *J. Chem. Phys.* **1942**, *10*, 428–440.
(31) Green-Church, K. B.; Limbach, P. A. *J. Am. Soc. Mass Spectrom.* **2000**, *11*, 24–32.

JP804786E